Articles in PresS. J Neurophysiol (June 30, 2010). doi:10.1152/jn.00393.2010

Repetition Suppression Dissociates Spatial Frames of Reference in Human Saccade Generation

Running title: Repetition suppression during saccade generation

Stan Van Pelt[1*], Ivan Toni[1], Jörn Diedrichsen[2], W. Pieter Medendorp[1]

[1]Radboud University Nijmegen, Donders Institute for Brain, Cognition and Behaviour, NL 6500 HE, Nijmegen, The Netherlands.
[2]University College London, Institute of Cognitive Neuroscience; 17 Queen Square, London WC1N 3AR, United Kingdom

*Corresponding author:
Radboud University Nijmegen
Donders Institute for Brain, Cognition and Behaviour
P.O. Box 9104, NL-6500 HE, Nijmegen
The Netherlands
Phone: +31 24 366 8495
FAX: +31 24 361 0989
Email: stan.vanpelt@donders.ru.nl

June 8, 2010 (revised version)

Figures: 6
Tables: 2
Pages: 36

Abstract

The path from perception to action involves the transfer of information across various reference frames. Here we applied an fMRI repetition suppression (RS) paradigm to determine the reference frame(s) in which the cortical activity is coded at several phases of the sensorimotor transformation for a saccade, including sensory processing, saccade planning and saccade execution. We distinguished between retinal (eye-centered) and non-retinal (e.g., head-centered) coding frames in three key regions: the intraparietal sulcus (IPS), frontal eye field (FEF) and supplementary eye field (SEF). Subjects (n=18) made delayed-saccades to one of five possible peripheral targets, separated at intervals of 9º visual angle. Target locations were chosen pseudo-randomly, based on a 2x2 factorial design with factors retinal and non-retinal coordinates and levels novel and repeated. In all three regions, analysis of the BOLD dynamics revealed an attenuation of the fMRI signal in trials repeating the location of the target in retinal coordinates. The amount of retinal suppression varied across the three phases of the trial, with the strongest suppression during saccade planning. The paradigm revealed only weak traces of non-retinal coding in these regions. Further analyses showed an orderly representation of the retinal target location, as expressed by a contralateral bias of activation, in the IPS and FEF, but not in the SEF. These results provide evidence that the sensorimotor processing in these centers reflects saccade generation in eye-centered coordinates, irrespective of their topographic organization.

Keywords: saccade generation, fMRI, reference frames, repetition suppression

Introduction

To understand how the brain processes and transforms spatial information for movements, the notion of a reference frame is indispensable (Soechting and Flanders 1992). Using this concept, electrophysiological evidence from the monkey has shown that movement-related neurons employ a variety of reference frames, anchored to eyes, head, other body-parts, or world (Colby 1998; Andersen and Buneo 2002; Martinez-Trujillo et al. 2004; Olson 2003). However, it is unclear to what extent this information, which is extracted from post-synaptic action potentials of a relatively small number of pyramidal neurons, can be related to the computations of larger neuronal populations (Logothetis 2008) and to other species, including humans.

Data on spatial reference frames of large neuronal assemblies in the human brain are still scarce. A few recent fMRI studies addressed this issue using topographic mapping procedures. Examining how topographic maps of target locations change as a function of eye position allows to distinguish between retinal (eye-centered) or non-retinal (head/body/space centered) reference frames (Medendorp et al. 2003; Merriam et al. 2003; Sereno and Huang 2006; Gardner et al. 2008). As a result, Medendorp et al. (2003) demonstrated the existence of a retinocentric saccade-and-reach area in parietal cortex, which was recently shown to code movement goals, not motor commands (Fernandez-Ruiz et al. 2007)

However, neurons may not always be topographically arranged along the dimensions of the reference frame they employ. A brain area could encode information in a particular reference frame even if the respective neurons do not show an orderly spatial organization according to the value of that particular

88 parameter. This is likely the case for regions involved in movement control,
89 where multidimensional motor constraints must be organized into a two-
90 dimensional map (Graziano and Aflalo 2007).

91 Repetition suppression (RS) offers a potential solution to investigate the
92 reference frames used in the neural control of movement without relying on the
93 special case of an orderly topographic arrangement of the relevant neurons. RS
94 is based on the observation that repeated processing of a given stimulus
95 feature leads to a reduction of neural activity in neurons tuned to that particular
96 feature (Desimone 1996). By varying the property of the stimulus across
97 different dimensions, the features processed in a given brain region can be
98 uncovered. While many fMRI studies have successfully used this technique in
99 studies of perceptual representation (McKyton et al. 2007; see Grill-Spector et
100 al. 2006, for review), expectation (Summerfield et al. 2008) and action
101 observation (Hamilton and Grafton 2006, 2008; Dinstein et al. 2008; Majdandžić
102 et al. 2009), to date this method has not been applied to examine neural
103 representations underlying sensorimotor control.

104 In this study, we used RS methods to investigate the reference frames
105 used to encode targets for saccadic movements in the main cortical centers for
106 saccades in the human brain: intraparietal sulcus (IPS), frontal eye field (FEF),
107 and supplementary eye fields (SEF). Participants executed memory-guided
108 saccades to peripherally presented target (Figure 1A). By varying the fixation
109 position for the next trial, we could then make the next target either identical in
110 retinal coordinates, or in non-retinal coordinates. We found a clear reduction of
111 the BOLD signal in all three regions on the second compared to the first trial
112 when the target location was repeated in retinal coordinates, but not, or much

less, during a repetition in a non-retinal frame. Retinal suppression was stronger during saccade planning than execution. This suggests that the neural commands from these centers, of which only some have a measurable topographic distribution of spatially-tuned neurons (IPS and FEF), encode saccade goals in retinocentric coordinates.

Materials and Methods

Subjects and ethical approval

Eighteen healthy subjects with normal or corrected-to-normal vision participated in the study (8 female, 10 male, aged 20-37 years). Three subjects were left-handed; one subject was aware of the exact purpose of the experiment. All gave written informed consent in accordance with the guidelines of the local ethics committee (CMO Committee on Research involving Human Subjects, region Arnhem-Nijmegen, The Netherlands). Subjects practiced the task 1-2 days in advance in a mock setup outside the scanner to ensure that the task and paradigm were correctly understood. In addition, a few practice trials were performed inside the scanner just prior to the experiment.

Experimental setup

Subjects were lying supine in the scanner, with their heads tilted 30° with respect to the scanner bed by means of a wooden support board that was attached to the bed. This enabled the subjects to view all stimuli directly without mirrors, making the task as natural as possible. Their head was fitted inside a phased-array receiver head coil. The head and neck were stabilized within the

head coil using foam blocks and wedges. A foam block was also placed underneath the knees, and in some subjects the elbows and neck were further supported by cushions to make them feel more comfortable.

A stimulus device consisting of seven horizontally placed yellow-colored light-emitting diodes (LEDs), was attached to an arch of about 40 cm height that was placed over the subject's hip, at a viewing distance of 34 cm. The central LED was aligned with the subject's body midline; three peripheral LEDs were located on either side, at an eccentricity of 4.5, 9 and 18° from the central LED. This configuration allowed subjects to view all stimuli with a comfortable, slightly downward gaze direction relative to the head.

Stimulus LEDs were controlled using Presentation software (Neurobehavioral Systems, San Fransisco, CA, USA). Position of the left eye was recorded using a long-range infrared video-based eyetracker (SMI, Teltow, Germany) at a frequency of 50 Hz.

MR settings

Anatomical and functional images were obtained on a Siemens 3 Tesla MRI scanner (Siemens Trio, Erlangen, Germany). Functional images consisted of 32 axial slices acquired by a gradient-echo planar imaging sequence using an eight-channel phased-array receiver head coil (slice thickness 3.0 mm, gap = 17%, in-plane pixel size 3.5 x 3.5 mm, TR = 2000 ms, TE = 35 ms, FOV = 224 mm, flip angle = 80°). In total, 1140 functional images were obtained in one run, lasting 35 minutes. Hereafter, high-resolution anatomical images were acquired using a T1-weighted MP-RAGE sequence (192 sagittal slices, voxel size 1.0 x 1.0 x 1.0 mm, TR = 2300 ms, TE = 2.02 ms, FOC = 256 mm, flip angle = 8°).

163

164 *Experimental paradigm*

165 The experiment took place in complete darkness; only the stimulus LEDs were
166 visible. Subjects performed a memory-guided saccade task, using a rapid
167 event-related repetition suppression (RS) design (Figure 1A, upper panel). A
168 trial started with a subject fixating an illuminated stimulus LED (Fixation Point,
169 F). Then, after a period of 3 s, one of the other stimulus LEDs flashed for 200
170 ms, which served as the target stimulus (S) for the pending saccade. This was
171 followed by a 3.8 s memory delay during which the subject maintained fixation
172 on F. Subsequently, F was extinguished, which was the go-cue for the subject
173 to make the saccade to S, as accurately as possible. Then, 1 s later, the next
174 trial started, with an intermediate refixation saccade to change F to a different
175 location than S in the previous trial. Each trial lasted eight seconds. Trial lengths
176 were not jittered to rule out potential confounding effects caused by the
177 nonlinear nature of RS (Van Turennout and Martin 2003). Furthermore, the trial
178 sequence was chosen such that correlation between the fMRI-regressors
179 describing the BOLD-signal during the delay period was low (<0.3). The total
180 experiment consisted of 36 blocks of 4 trials, yielding a total of 144 trials.

181 In each trial, both F and S could be presented at one of five possible
182 locations, at -18°, -9°, 0°, +9° or +18° from the center. Combinations of F and S
183 were chosen pseudo-randomly; we did not test trials in which S=F since this
184 implied no saccadic response. In the majority of trials (85 %), the angular
185 separation between F and S was 9° to exploit the fact that 9° saccades may
186 drive higher BOLD responses than larger amplitude saccades, based on the

overrepresentation of the central visual field in several visual and oculomotor regions (Ben Hamed et al. 2001).

Because the head and body were fixed during the experiment, head, body, and space-centered reference frames can be treated as equivalent, and are therefore referred to as a non-retinal reference frame. Likewise, under the present conditions, retinocentric, eye-centered and gaze-centered reference frames can be considered synonymous notions, and referred to as a retinal reference frame.

Repetition suppression effects were elicited by systematically manipulating target location over successive trials in a 2x2 design, with conditions retinal and non-retinal coordinates (labeled as R and N, respectively), and levels novel and repeated (labeled as n and r, respectively). E.g., as illustrated in Figure 1A, the retinal location of a target presented in trial t, could be repeated in the next trial t+1, while the non-retinal location was novel (lower left panel; retinal repeated, non-retinal novel; RrNn). Alternatively, the retinal location of the target in trial t+1 could be novel compared to the preceding trial t, while the non-retinal location was repeated (RnNr, lower right panel). Finally there were two types of trials (not shown) in which the location of the target was either repeated or novel in both coordinate frames (RrNr and RnNn, respectively).

The first trial of each block was not included in the RS analysis in order to avoid carry-over effects from the previous block (we used these trials to define our oculomotor regions-of-interest, see below). The remaining 108 trials consisted of 36 RnNn trials, and 24 trials of each of the other three types of trials (RrNn, RnNr, RrNr). A target's retinal or non-retinal location was never

212 repeated more than once in a row in order to get the strongest RS effects and
213 avoid adaptation fatigue (Van Turennout et al. 2003). Target directions were
214 balanced across the visual and craniotopic hemifields; average amplitudes were
215 the same across the four conditions. The intermediate saccades between trials
216 to change initial fixation points were also chosen such that on average they
217 could not explain any RS effect in either reference frame.

218 After each block of four trials, subjects performed a so-called washout
219 task to allow the BOLD signal to return to baseline level after several RS trials,
220 alleviating possible longer lasting RS effects (Majdandžić et al. 2009). The start
221 of this washout task was indicated by three brief subsequent flashes of two
222 targets (first -4.5°/+4.5°, then -9°/+9°, finally -18°/18°), followed by the onset of
223 the central LED for a jittered duration (1.4-12.6 s). Subjects were instructed to
224 fixate this LED and track it as it subsequently jumped to different locations after
225 each 250 ms, eight times in total. These locations were balanced across
226 directions and were evenly distributed across the 7 LEDs on the stimulus
227 device. The washout task ended by a period of central fixation (1.4-14.0 s)
228 followed by again the same three short flashes, but now in opposite order. Each
229 washout period lasted 15.2 – 32.0 s (mean 23.1 s). After each 6 blocks and
230 their associated washouts, subjects had a rest period of 30 s, during which
231 there was no visual stimulation and they could freely move their eyes. The total
232 experiment lasted 60 minutes, including practice and anatomical scanning.

233

234 *Behavioral analysis*

235 Eye movement data (horizontal component) were processed separately per
236 block of four trials and calibrated in degrees based on the fixation data of the

following washout period. This generally yielded calibration accuracies better than 1.5°. Figure 1B show the eye traces of a typical subject from central fixation to a remembered target location at either 9° (gray) or -9° (black), in relation to the temporal order of events (see Fig 1A). As shown, this subject maintained fixation during the presentation of the target cue, and made eye movements with latencies of about 200 ms in the correct directions after the fixation target was turned off. Due to technical problems, eye-movement data of one subject were lost for the last 12 blocks of trials. We used the eye recordings to identify error trials, which were defined as trials in which subjects did not keep fixation when required, or made saccadic responses that were anticipatory or into the wrong direction. Although the temporal resolution (20 ms) was relatively course, eye traces were also used to determine reaction times. On average, 9 ± 4 (SD) trials per subject were discarded based on these criteria. For the remaining trials, average fixation accuracy was 1.8° (SD = 1.4°) across subjects. Accuracy of saccades to the remembered targets, in degrees of visual angle, was 3.0° (SD = 1.2°) across conditions. This confirmed that the saccades were driven by the memory of the actual targets and were not simply guided stereotypically to the left or right.

Preprocessing of fMRI data

fMRI data were analyzed using BrainVoyager QX (Brain Innovation, Maastricht, The Netherlands). Subsequent analyses were performed using Matlab (The Mathworks). The first five volumes of each subject's data set were discarded to allow for T1 equilibration. Functional data were first corrected for slice scan time acquisition and motion. Subsequently, the data were temporally filtered using a

262 high-pass filter with a cutoff frequency of 1/268 s. The functional images were
263 co-registered with the anatomical scan and transformed into Talairach
264 coordinate space using the nine-parameter landmark method (Talairach and
265 Tournoux 1988). Finally, the images were smoothed with an isotropic Gaussian
266 kernel of 8-mm full-width-at-half-maximum.
267
268 *Statistical inference and regions of interest*
269 The goal of the study is to use repetition suppression to investigate the
270 reference frames employed in the three key cortical centers for saccades; the
271 IPS, FEF and SEF. We used the first trials (referred to below as localizer trials)
272 of each block to identify these regions, while the other trials (below referred to
273 as RS trials) in the block subserved the RS analysis in the regions. This split of
274 the data was done to avoid any circular analyses of the data (see Kriegeskorte
275 et al. 2009).
276 For each subject we defined 19 regressors. Four of these were used in
277 relation to localizing the ROIs. More specifically, one regressor specified the 2-s
278 fixation period of the localizer trials as well as the fixation periods in the washout
279 task, the second, third and fourth regressors specified the stimulus period, the
280 memory interval and the saccade periods of the localizer trials.
281 Seven regressors were modeled in relation to studying the RS effects,
282 based on using the RS trials. The first modeled the 2-s fixation periods at the
283 beginning of each trial. The second regressor captured the periods of 0.2 s
284 during which the target stimulus was presented. Four other regressor functions
285 characterized the subsequent working memory interval according to the 2 x 2
286 design of conditions Retinal (R) and Non-retinal (N) locations with levels Novel

287 (n) and Repeated (r). These regressors (RnNn, RrNn, RnNr, and RrNr) covered
288 the 3.8 s delay period starting with target offset until fixation point offset (go
289 cue). Saccade periods of the RS trials were modeled by the seventh regressor,
290 which included the first second after the go cue and the first second after
291 presentation of the fixation LED of the next RS trial.

292 In addition to these eleven regressors, we used eight regressors of non-
293 interest. One modeled the delay periods of error trials; another characterized
294 the periods of rest and the intervals in which the cues for the start and end of
295 the washout period were presented. All regressors were defined as boxcar-
296 functions over the time interval they described and were convolved with a
297 hemodynamic response function (modeled using a two-gamma model function
298 with response undershoot ratio of 6, time to response peak of 5 s and time to
299 undershoot peak of 15 s). The final six regressor functions represented the
300 head motion, based on the six parameters provided by BrainVoyager's motion-
301 correction algorithm.

302 Individual subject GLMs were corrected for serial correlations in the time
303 courses. Random effects group analyses were performed to test effects across
304 subjects, using the false discovery rate (FDR) controlling procedure to correct
305 for multiple comparisons, at the q(FDR)<0.01 significance level (Genovese et al.
306 2002). Using a random-effects group analysis, we first determined the regions
307 that show significant activity during oculomotor preparation and execution in the
308 localizer trials. From the activation maps, we selected three bilateral regions of
309 interest (ROI), known to be important regions in saccade generation: FEF, SEF
310 and a region in the intraparietal sulcus (IPS). Each ROI was defined as all the
311 contiguous voxels that exceeded a threshold of q(FDR)<0.05 within a cubic

312 cluster of 8x8x8 mm (to match the smoothing kernel), centered at the points of
313 peak activation.
314
315 *Linear deconvolution*
316 In a second analysis, we used finite impulse response deconvolution to extract
317 the activation profiles in the ROIs for each of the four RS conditions (RnNn,
318 RrNn, RnNr, and RrNr). In this approach, the BOLD data were first resampled
319 into 0.5 s time intervals. Then, for each condition, a set of 31 impulse responses
320 (one impulse per 0.5-s volume) was aligned to the start of each trial in the
321 group. Together, the 31 impulse regressors for a given condition modeled the
322 activation time course for trials in this condition with two points per second over
323 15 s. Thus, each group of trials yielded 31 columns to a subject's GLM design
324 matrix, with ones at the appropriate locations, to model the 31 impulse functions
325 for that trial group (Dale 1999; Serences 2004; Brown et al. 2006). Fitting this
326 design matrix to the resampled data automatically deconvolves the time series
327 of each RS condition (Brown et al. 2006), without making any assumption about
328 the shape of the activation profile, other than its length (15 s in this case).
329 Because of the random ordering of the four trial types, effects of previous trials
330 are balanced out in this analysis (is assumed that the haemodynamic response
331 is linear), as is shown in Fig 3, where all time traces start from the same
332 baseline. Next, for each RS condition and each ROI, a mean signal and
333 standard deviation were computed across subjects. Differences between
334 conditions capture the RS effects in either reference frame. That is, retinal RS
335 follows from (RnNn + RnNr) – (RrNn + RrNr) and non-retinal RS is computed as

336 (RnNn + RrNn) – (RnNr + RrNr). Statistical significance was tested using paired
337 t-tests and repeated-measures ANOVAs at the $P<0.05$ confidence level.
338
339 **Results**
340
341 *Behavioral performance*
342 Subjects performed memory guided saccades to targets whose coordinates
343 were systematically manipulated in both retinal and non-retinal coordinates
344 (labeled as R and N, respectively). Thus, with respect to the previous trial,
345 target locations could be novel in both retinal and non-retinal coordinates
346 (RnNn, see Figure 1A), repeated in both reference frames (RrNr), or novel in
347 one, but repeated in the other frame (RnNr and RrNn).
348 Table 1 shows performance (defined as correct fixation and saccade
349 direction) and saccade latencies for each of these four trial types. Across
350 subjects, performance was >93% correct, in all conditions. A 2x2 repeated-
351 measures ANOVA with repeated versus non-repeated trials and retinal versus
352 non-retinal target locations as factors revealed no significant main
353 ($F(1,17)<3.98$, $P>0.062$) or interaction effect ($F(1,17)=1.30$, $P=0.27$). The mean
354 latency of the saccadic response was 217 $\pm$ 69 ms (mean + SD) across the four
355 conditions. The differences among the four conditions were not statistically
356 significant ($F(1,17)<0.86$, $P>0.36$). Finally, there were no differences either in
357 performance or in saccadic latency between the first and second half of the
358 performed trials (t-test, $P<0.01$). Together, the behavioral results indicate that
359 possible differences in corresponding fMRI activations cannot be related to
360 different levels of task performance.

361

362 *fMRI activation data*

363

364 *Activation maps during delay period*

365 Using a random-effects group GLM analysis across all 18 subjects, we first
366 identified the cortical areas involved in saccade generation using the localizer
367 trials (see Methods). Figure 2A and B show two anatomical views of these
368 results, in neurological convention, thresholded at q(FDR)<0.01. In Fig 2C and
369 D, this activation map is rendered onto an inflated representation of the left
370 hemisphere of one of the subjects. Consistent with previous results, a bilateral
371 network of eye-movement related cortical areas was activated (Schluppeck et
372 al. 2005; Curtis and D'Esposito 2006; Brown et al. 2004; Connolly et al. 2002).
373 This included a region along the intraparietal sulcus (IPS), which might be the
374 human analog of monkey area LIP (Medendorp et al. 2003; Connolly et al.
375 2007; Sereno et al. 2001). In the frontal cortex, we found significant voxels at
376 the junction of the precentral sulcus and the superior frontal sulcus, probably
377 corresponding to the frontal eye field (FEF; Paus et al. 1996; Brown et al. 2004).
378 More medially, significant voxels were found along the interhemispheric fissure,
379 extending onto the dorsal cortical surface, which can be classified as the
380 supplementary eye field (SEF; Picard and Strick 2001; Grosbras et al. 1999;
381 Brown et al. 2004). Finally, more laterally in the left frontal cortex, significant
382 responses were found in voxels covering the precentral sulcus, corresponding
383 to the ventral premotor area (PMv; Picard and Strick 2001; Beurze et al. 2007).

384 Table 2 lists the mean Talairach coordinates (in mm) of the peak voxel
385 within each region, together with the corresponding t-values across subjects.

386 From these regions, we subjected the bilateral regions IPS, FEF, and SEF,
387 each defined as all contiguous voxels exceeding a threshold of q(FDR)<0.05
388 within a cubic cluster of 8x8x8 mm, to a careful investigation of the RS effects.
389
390 *Reference frame-dependent repetition suppression*
391 Can repetition suppression reveal which frames of reference are used to code
392 the representation in these oculomotor regions? Given our hypotheses, we may
393 predict that, when the retinal location of a target is repeated in subsequent
394 trials, voxels will show an attenuation of their BOLD-activation when the
395 underlying neuronal populations code target location in a retinal reference
396 frame, but not if they code in a non-retinal reference frame. Conversely, regions
397 that code the non-retinal (e.g. craniotopic) location of a target will only show
398 BOLD adaptation when the non-retinal location of the target is repeated. Of
399 course, it is also possible that a region would be best characterized by a mixture
400 of these two frames.
401 Figure 3A shows the reconstructed BOLD response of the left and right
402 IPS over a time course of 12 s, averaged across subjects (see Methods).
403 Repeated trials (gray) had the same target location as the previous trial (black)
404 in retinal coordinates. Time t=0 s denotes the onset of the target stimulus; t=4 s
405 the go-cue for the saccade. As shown, in both novel and repeated trials, after
406 the brief presentation of the target stimulus (t=0 s), cortical activation during the
407 first delay period shows first a phasic response (time interval 0 to 4 s), followed
408 by a tonic response (time 4 - 6 s). Then, at time 7 - 10 s, there is again a strong
409 increase in cortical activation, caused by the execution of planned saccade and
410 the subsequent saccade to fixate a new fixation point (see Methods). The

411 activity, in particular the early phasic and tonic activity is suppressed in
412 repeated trials compared to novel trials, in both hemispheres, which would be
413 consistent with the prediction of the retinal model. Figure 3C illustrates this
414 more clearly, by showing the mean difference (± 95% confidence intervals)
415 between the activation patterns during novel and repeated trials (average
416 repetition suppression in retinal coordinates). Across the entire trial period,
417 BOLD activation during repeated trials is significantly lower than during novel
418 trials (paired t-test, $P<0.001$), with the suppression effects most pronounced
419 during the tonic delay phase.

420 To investigate whether the retinal representation in the IPS is
421 intermingled with a non-retinal representation, we compared novel and repeated
422 trials with the same target location in non-retinal coordinates. As shown in
423 Figure 3B, activation patterns during novel and repeated trials are quite similar.
424 Their difference is plotted in Fig 3D, together with the 95% confidence intervals
425 (gray area). Across the entire time course, and in both hemispheres, the
426 difference in activation does not significantly deviate from zero ($P>0.41$). Thus,
427 we found no clear evidence for a non-retinal representation, in contrast to clear
428 findings regarding the retinal representation.

429 The results of the IPS are exemplary for those in the FEF and SEF.
430 Therefore, to analyze the findings quantitatively for each ROI, we computed in
431 each subject the average difference between the novel and repeated signals at
432 three phases of the trial, indicated by the vertical gray boxes in Figure 3A. The
433 resulting value is a measure for the amount of repetition suppression (RS
434 value). We computed these RS values (corrected for the fMRI hemodynamic
435 lag) for the stimulus-related activity (S: 1-3.5 s), the delay period (D: 4-6.5 s),

436 and the execution phase (E: 7.5-10 s). For each ROI, the amount of RS was
437 determined across hemispheres, in both reference frames.

438 Figure 4 plots the average results of this analysis across the entire group
439 of subjects. As shown, brain activations are significantly suppressed when a
440 target location is repeated in retinal coordinates (black bars), for all ROIs and
441 trial phases (repeated measures ANOVA; $F(1,17)>5.5$, $P<0.05$ in all cases).
442 Retinal suppression was strongest during the delay phase. This confirms the
443 observations in Figure 3 and illustrates the role of these regions in saccade
444 planning. In contrast, we found only weak, non-significant suppression effects
445 when a target location is repeated in non-retinal coordinates (white bars) during
446 the delay phase, and not during the stimulus or execution phases.

447 The current design was not sensitive enough to test a potential
448 magnitude effect of increasing RS with saccade size, because the set of
449 saccades with amplitudes larger than 9° was too small (15%). Such an effect
450 could be expected on basis of the cortical magnification of the central visual
451 field in the early cortical stages of processing However, when we constrained
452 our analysis to only the trials with 9° saccades, the retinal RS values were not
453 significantly different compared to including all trials. This was the case for all
454 areas and trial epochs ($P>0.05$).

455 To test how much these results hold within single subjects, we
456 determined a reference frame index (RFI) on basis of the RS effects for each of
457 them. This index value was computed as the difference between the amount of
458 retinal and non-retinal RS, weighted by their cumulative effect size. The
459 histograms in Fig 5 show the distribution of these RFIs across subjects. For all
460 regions and trial phases, there is a clear bias in the population of subjects

461 towards retinal coding. This is reflected in the average RFI, which is in all cases
462 significantly larger than zero ($P<0.01$), with values varying between 0.21 ± 0.30
463 (mean ± SD) (SEF, delay period) and 0.36 ± 0.36 (SEF, execution phase).
464 Together, the results presented in Figs 4 and 5 provide evidence for the
465 existence of, at least, a dominant sustained eye-centered representation in the
466 selected saccade regions.
467
468 *Contralateral bias*
469 To what extent are the RS findings of a retinal coding of target location
470 consistent with the topographic organization of these areas, as revealed by
471 lateralized cortical activity? Because we varied eye position, our paradigm
472 allows us to distinguish between lateralized activity in retinal and non-retinal
473 coordinates. If the spatially-selective retinal neurons are topographically
474 organized in the selected ROIs, we would expect that targets in the contralateral
475 visual field will generate a higher BOLD response than targets presented in the
476 ipsilateral hemifield. Alternatively, it is possible that the retinal RS effects are not
477 embedded in a neural map with an orderly spatial organization. Because only
478 retinal RS effects were seen, we anticipate that none of the regions will
479 demonstrate non-retinal laterality.
480 To test the presence of lateralized activity in our data, we performed two
481 GLM analyses, each using two regressors to describe target location (left or
482 right in retinal or non-retinal coordinates) during the delay period (see also
483 Methods). We compared the resulting beta-weights of these regressors in both
484 GLMs, separately for each ROI. Figure 6A presents the differences between the
485 activity elicited by contralateral and ipsilateral targets. For the IPS and FEF, a

strong contralateral bias was found, in retinal coordinates, which was significant across hemifields (repeated measures ANOVA; $F(1,17)>28.4$, $P<0.001$ in both regions). In the SEF, however, there was no significant lateralized activity ($F(1,17)=0.08$, $P=0.78$). In combination with our RS results, this suggests that, although retinal RS effects are present in the SEF, there is no contralateral bias of these spatially selective neurons in this area.

For completeness, when targets were sorted according to their non-retinal (head-centric) location, there was no significant difference between contralateral and ipsilateral activity in any of the regions (Figure 6B; repeated measures ANOVA; $F(1,17)<1.6$; $P>0.22$ in all regions). This compares well to the RS results, which do not favor the non-retinal reference frame either.

All together, our results show that repetition suppression can be used as a tool to distinguish between reference frames in frontoparietal areas involved in spatial memory processing for saccades, even when those regions lack a clear topographic organization.

Discussion

Identifying the computational architecture of the human brain has been a major aim in neuroscience research over the last decades. One of the key questions concerns the internal organization of the various brain regions involved in sensorimotor processing, i.e., how and why different regions provide different solutions to the underdetermined problem of mapping multidimensional motor constraints into a two-dimensional neuronal matrix (Graziano and Aflalo 2007; Kohonen 2001).

510 Using repetition suppression (RS) effects, we addressed a particular
511 instance of this general issue by studying the spatial reference frames
512 employed by three human oculomotor areas (IPS, FEF, and SEF) in the context
513 of a delayed-saccade task (Pierrot-Desilligny et al. 2004). Subjects performed
514 trials of delayed-saccades that were repeated with the remembered target at
515 the same location in either retinal or non-retinal coordinates. Within all regions,
516 significant suppression effects were observed in relation to repetition of the
517 target location in retinal coordinates (Figures 3-5). We found the time course of
518 retinal suppression to show the strongest attenuation effects during the delay
519 period, reflecting the important role of these regions in preparing the saccade.
520 Slight non-retinal suppression effects were observed during the delay interval
521 only, but these did not reach statistical significance.

522 We also investigated the lateralization of activity in the hemispheres
523 when targets were presented ipsi- or contralateral in either retinal (eye-
524 centered) or non-retinal (head/body/space centered) coordinates. This revealed
525 a bias to contralateral target locations in the IPS and FEF, defined in reference
526 to the eye, which is consistent with the retinal repetition suppression effects (Fig
527 6). We emphasize that the clear laterality found in the IPS and FEF should not
528 be taken to imply that the areas do no respond to ipsilateral targets, but just that
529 the response is stronger on the contralateral side. This also explains why we
530 found retinal suppression effects in both hemispheres (Fig 3).

531 These findings confirm previous fMRI results on the topographic
532 representation of saccadic movements in IPS and FEF (Sereno et al. 2001;
533 Schluppeck et al. 2005; Kastner et al. 2007; Hagler and Sereno 2006;
534 Medendorp et al. 2006; Curtis and D'Esposito 2006; Curtis and Connolly 2008).

535 Medendorp et al. (2003) exploited the topography to demonstrate the updating
536 of parietal activation when an eye movement changes the remembered location
537 a visual target across hemifields. The present findings are also fully consistent
538 with the coding of such a dynamic retinocentric representation, providing a
539 novel empirical validation of the RS method for studying the motor system.

540 Our data provides no evidence for a contralateral activation bias in the
541 SEF, in either retinal or non-retinal coordinates (see Fig 6), which is consistent
542 with recent fMRI findings by Kastner et al. (2007). Nevertheless, just as LIP and
543 FEF, the human SEF appears to encode saccadic movements in a retinocentric
544 frame of reference (see Figs 4 and 5). These findings illustrate that, whereas
545 these three visuomotor areas process eye-centered saccadic information, their
546 topographic layouts suggest different use of this information. Under the
547 assumption that the structural organization of the cerebral cortex follows the
548 principle of maximizing smoothness of neurally encoded features (Graziano and
549 Aflalo 2007; Durbin and Mitchison 1990), we infer that spatial features constitute
550 a relevant dimension for IPS and FEF computations and not for the SEF, in line
551 with a role of the latter region in operational saccade regulation (Stuphorn et al.
552 2009), guiding eye movements according to arbitrary sets of visual elements
553 (Olson 2003; Berdyyeva and Olson 2009), and stimulus-response associations
554 (Chen and Wise 1996; see Nachev et al. 2008, for a review).

555 In support of our interpretations, the virtual absence of non-retinal
556 suppression effects indicates that the observed retinal suppression effects
557 cannot be due to general motor habituation or fatigue, but mark the identity of
558 the underlying neural organization. It has been proposed that RS may be the
559 result of a ‘sharpening’ of cortical representations (Wiggs and Martin 1998;

560 Desimone 1996; Grill-and Malach 2001; Vidyasagar et al. 2010). A repeating
561 stimulus can be coded more efficiently by employing fewer active neurons
562 (Desimone 1996; Friston 2005). From a Bayesian perspective (Ma et al. 2006;
563 Vaziri et al. 2006), this can be understood in terms of a target location of the last
564 trial serving as a prior probability distribution for the next trial. When this prior is
565 integrated with the new sensory evidence, the network may settle to a tighter
566 distribution in neural space at the second repetition.

567 Notably, we certainly do not want to claim that the practical absence of
568 non-retinal suppression indicates the absence of non-retinal coding in the brain.
569 We cannot exclude that the non-retinal repeat trials induced a different form (i.e.
570 timing) of adaptation, which we did not detect. Alternatively, this absence may
571 also relate to our paradigmatic constraints, testing saccades to remembered
572 visual targets. Other effector systems (e.g. reaching) and sensory modalities
573 may reveal clear non-retinal suppression effects, but this is something to be
574 pursued in future experiments.

575 Apart from revealing spatial reference frames, the transient dynamics of
576 RS during the trial is further informative about functional specialization in the
577 various regions. The stronger suppression effect during the delay period as
578 compared to the stimulation period and execution phase (Fig 4 and 5) suggests
579 a more important role in preparing the saccade than in processing the sensory
580 aspects of the target. Suppression is also much stronger during planning than
581 during execution of the eye movement. For eye movement execution, eye-
582 centered representations must be further transformed, as a function of eye
583 position, by downstream mechanisms into head-centered (non-retinal)
584 commands for the ocular muscles (Crawford and Guitton 1997). As Figures 3-5

585 show, we did not observe clear non-retinal suppression effects in these regions.
586 To explain this, it is important to realize that two physically identical eye
587 movements require also the same patterns of muscle innervations. Thus
588 saccade execution would simply not allow for any suppression of activity at the
589 neuromuscular level. But as our data show, resemblance of this notion is found
590 even at the cortical level, reflecting a network that is involved in both planning
591 and executing the movement.

592 When comparing our results to monkey neurophysiological findings, we
593 should keep in mind that BOLD-imaging mostly reflects the pre-synaptic activity
594 summed over a large number of neurons (Logothetis 2008; Bartels et al. 2008),
595 whereas single unit recording reports about the output stage of those
596 computations. Despite these reservations, the present findings are for the most
597 part quite consistent with previous neurophysiological experiments in monkeys
598 (Koyama et al. 2004). Among these are studies which report evidence for an
599 retinocentric topographic organization of saccade targets in the lateral
600 intraparietal sulcus (Blatt et al. 1990; Colby 1998; Ben Hamed et al. 2001) and
601 the FEF (Bruce and Goldberg 1985; Robinson and Fuchs 1969; Schall 1991).
602 Although many earlier human studies have reported topographic maps in the
603 IPS and FEF (see above), the underlying reference frame has been much less
604 studied. The present study, examining the spatial organization across different
605 eye positions, provides solid evidence for a retinocentric topographic
606 organization of both regions.

607 Debate exists about a topographic organization of saccade goals in
608 monkey SEF (Schlag and Schlag-Rey 1987, Tehovnik and Lee 1993; Russo
609 and Bruce 2000). Various single-unit studies have provided evidence that SEF

610 neurons can encode target locations in a continuum from eye-, to head-, to
611 body- and object-centered reference frames (Martinez-Trujillo et al. 2004; Olson
612 2003; Schlag and Schlag-Rey 1987), perhaps to represent all possible
613 contingencies for different task-related motor functions (Martinez-Trujillo et al.
614 2004). In contrast, our study has revealed a strong bias towards retinal coding
615 in the human SEF, and the lack of contralateral activation bias indicated a clear
616 absence of topographic structure. In addition to the methodological differences
617 stated above (single-units vs fMRI, see Logothetis 2008), another possible
618 explanation for the apparent discrepancy is that the head-fixed saccade
619 conditions here have constrained us probing representations other than those
620 referenced to the eyes (see also the argument above).

621 In conclusion, the present study exploited fMRI-RS to unveil the frames
622 of reference employed by frontal and parietal areas during saccade planning.
623 While our findings advance the understanding of how the human brain
624 processes spatial information for saccades, they also support the feasibility and
625 validity of using RS methodology in the sensorimotor domain.

626

627 **Acknowledgements**

628 The authors thank Paul Gaalman and Jasminka Majdandžić for assistance
629 during the experiments. Address correspondence to email:
630 stan.vanpelt@donders.ru.nl.

631

632 **Grants**

633 This work was supported by the Netherlands Organisation for Scientific
634 Research (grant NWO-VIDI 452.03.307), and the Human Frontier Science
635 Program (CDA) to W.P.M.
636
637

638 **References**

639

640 **Andersen RA, Buneo CA.** Intentional maps in posterior parietal cortex. *Annu*
641 *Rev Neurosci* 25:189-220, 2002.

642 **Bartels A, Logothetis NK, Moutoussis K.** fMRI and its interpretations: an
643 illustration on directional selectivity in area V5/MT. *Trends Neurosci* 31:
644 444-453, 2008.

645 **Ben Hamed S, Duhamel JR, Bremmer F, Graf W.** Representation of the visual
646 field in the lateral intraparietal area of macaque monkeys: a quantitative
647 receptive field analysis. *Exp Brain Res* 140: 27-44, 2001

648 **Berdyyeva TK, Olson CR.** Monkey supplementary eye field neurons signal the
649 ordinal position of both actions and objects. *J Neurosci* 29: 291-299, 2009.

650 **Beurze SM, de Lange FP, Toni I, Medendorp WP.** Integration of target and
651 effector information in the human brain during reach planning. *J*
652 *Neurophysiol* 97: 88-99, 2007.

653 **Blatt GJ, Andersen RA, Stoner GR.** Visual receptive field organization and
654 cortico-cortical connections of the lateral intraparietal area. area LIP. in the
655 macaque. *J Comp Neurol* 299: 421-445, 1990.

656 **Brown MR, DeSouza JF, Goltz HC, Ford K, Menon RS, Goodale MA,**
657 **Everling S.** Comparison of memory- and visually guided saccades using
658 event-related fMRI. *J Neurophysiol* 91: 873-889, 2004.

659 **Brown MR, Goltz HC, Vilis T, Ford KA, Everling S.** Inhibition and generation
660 of saccades: rapid event-related fMRI of prosaccades, antisaccades, and
661 nogo trials. Neuroimage 33: 644-659, 2006.

662 **Bruce CJ, Goldberg ME.** Primate frontal eye fields. I. Single neurons
663 discharging before saccades. *J Neurophysiol* 53: 603-635, 1985.
664 **Chen LL, Wise SP.** Evolution of directional preferences in the supplementary
665 eye field during acquisition of conditional oculomotor associations. *J*
666 *Neurosci* 16: 3067-3081, 1996.
667 **Churchland MM, Afshar A, Shenoy KV.** A central source of movement
668 variability. *Neuron* 52: 1085-1096, 2006.
669 **Colby CL.** Action-oriented spatial reference frames in cortex. *Neuron* 20: 15-24,
670 1998.
671 **Connolly JD, Goodale MA, Menon RS, Munoz DP.** Human fMRI evidence for
672 the neural correlates of preparatory set. *Nat Neurosci* 5: 1345-1352, 2002.
673 **Connolly JD, Goodale MA, Cant JS, Munoz DP.** Effector specific fields for
674 motor preparation in the human frontal cortex. *NeuroImage* 34: 1209-1219,
675 2007.
676 **Crawford JD, Guitton D.** Visual-motor transformations required for accurate
677 and kinematically correct saccades. *J Neurophysiol* 78: 1447-1467, 1997.
678 **Curtis CE, Connolly JD.** Saccade preparation signals in the human frontal and
679 parietal cortices. *J Neurophysiol* 99: 133-145, 2008.
680 **Curtis CE, D'Esposito M.** Selection and maintenance of saccade goals in the
681 human frontal eye fields. *J Neurophysiol* 95: 3923-3927, 2006.
682 **Dale AM.** Optimal experimental design for event-related fMRI. *Hum Brain Mapp*
683 8: 109-114, 1999.
684 **Desimone R.** Neural mechanisms for visual memory and their role in attention.
685 *Proc Natl Acad Sci* 93: 13494-13499, 1996.

686 **Dinstein I, Hasson U, Rubin N, Heeger DJ.** Brain areas selective for both
687 observed and executed movements. *J Neurophysiol* 98: 1415-1427, 2007.
688 **Durbin R, Mitchison G.** A dimension reduction framework for understanding
689 cortical maps. *Nature* 343: 644-647, 1990.
690 **Fernandez-Ruiz J, Goltz HC, DeSouza JF, Vilis T, Crawford JD.** Human
691 parietal "reach region" primarily encodes intrinsic visual direction, not
692 extrinsic movement direction, in a visual motor dissociation task. *Cereb*
693 *Cortex* 10:2283-2292, 2007.
694 **Friston K.** A theory of cortical responses. *Philos Trans R Soc Lond B Biol Sci*
695 360:815-836, 2005.
696 **Gardner JL, Merriam EP, Movshon JA, Heeger DJ.** Maps of visual space in
697 human occipital cortex are retinotopic, not spatiotopic. *J Neurosci* 28:
698 3988-3999, 2008.
699 **Genovese CR, Lazar NA, Nichols T.** Thresholding of statistical maps in
700 functional neuroimaging using the false discovery rate. *Neuroimage* 15:
701 870-878, 2002.
702 **Grefkes C, Ritzl A, Zilles K, Fink GR.** Human medial intraparietal cortex
703 subserves visuomotor coordinate transformation. *Neuroimage* 23: 1494-
704 1506, 2004.
705 **Grill-Spector K, Malach R.** fMR-adaptation: a tool for studying the functional
706 properties of human cortical neurons. *Acta Psychologica* 107: 293-321,
707 2001.
708 **Grill-Spector K, Henson R, Martin A.** Repetition and the brain: neural models
709 of stimulus-specific effects. *Trends Cogn Sci* 10: 14-23, 2006.

710 **Graziano MS, Aflalo TN.** Mapping behavioral repertoire onto the cortex.
711 *Neuron* 56: 239-251, 2007.
712 **Grosbras MH, Lobel E, Van de Moortele PF, Lebihan D, Berthoz A.** An
713 anatomical landmark for the supplementary eye fields in human revealed
714 with functional magnetic resonance imaging. *Cereb Cortex* 9: 705-711,
715 1999.
716 **Hagler DJ Jr, Sereno MI.** Spatial maps in frontal and prefrontal cortex.
717 *Neuroimage* 29: 567-577, 2006.
718 **Hamilton A, Grafton S.** Goal representation in human anterior intraparietal
719 sulcus. *J Neurosci* 6: 1133-1137, 2006.
720 **Hamilton AF, Grafton ST.** Action outcomes are represented in human inferior
721 frontoparietal cortex. *Cereb Cortex* 18: 1160-1168, 2008.
722 **Jack AI, Patel GH, Astafiev SV, Snyder AZ, Akbudak E, Shulman GL,**
723 **Corbetta M**. Changing human visual field organization from early visual to
724 extra-occipital cortex. *PLoS ONE* 2: e452, 2007.
725 **Kastner S, DeSimone K, Konen CS, Szczepanski SM, Weiner KS,**
726 **Schneider KA.** Topographic maps in human frontal cortex revealed in
727 memory-guided saccade and spatial working-memory tasks. *J*
728 *Neurophysiol* 97: 3494-3507, 2007.
729 **Kohonen, T.** *Self-Organizing Maps.* Berlin (Germany): Springer, 2001.
730 **Koyama M, Hasegawa I, Osada T, Adachi Y, Nakahara K, Miyashita Y.**
731 Functional magnetic resonance imaging of macaque monkeys performing
732 visually guided saccade tasks: comparison of cortical eye fields with
733 humans. *Neuron* 41: 795-807, 2004.

Kriegeskorte N, Simmons WK, Bellgowan PSF, Baker CI. Circular analysis in systems neuroscience: the dangers of double dipping. *Nat Neurosci* 12: 535-540, 2009.

Logothetis NK. What we can do and what we cannot do with fMRI. *Nature* 453: 869-878, 2008.

Ma WJ, Beck JM, Latham PE, Pouget A. Bayesian inference with probabilistic population codes. *Nat Neurosci* 9: 1432-1438, 2006.

Majdandžić J, Bekkering H, van Schie HT, Toni I. Movement-specific repetition suppression in ventral and dorsal premotor cortex during action observation. *Cereb Cortex* 19: 2736-2745, 2009.

Martinez-Trujillo JC, Medendorp WP, Wang H, Crawford JD. Frames of reference for eye-head gaze commands in primate supplementary eye fields. *Neuron* 44: 1057-1066, 2004.

McKyton A, Zohary E. Beyond retinotopic mapping: the spatial representation of objects in the human lateral occipital complex. *Cereb Cortex* 17: 1164 – 1172, 2007.

Medendorp WP, Goltz HC, Vilis T, Crawford JD. Gaze-centered updating of visual space in human parietal cortex. *J Neurosci* 23: 6209–6214, 2003.

Medendorp WP, Goltz HC, Vilis T. Directional selectivity of BOLD activity in human posterior parietal cortex for memory-guided double-step saccades. *J Neurophysiol* 95: 1645-1655, 2006.

Merriam EP, Genovese CR, Colby CL. Spatial updating in human parietal cortex. *Neuron* 39: 361-373, 2003.

Nachev P, Kennard C, Husain M. Functional role of the supplementary and pre-supplementary motor areas. *Nat Rev Neurosci* 9: 856-869, 2008.

759 **Olson CR.** Brain representation of object-centered space in monkeys and
760 humans. *Annu Rev Neurosci* 26: 331-354, 2003.
761 **Paus T.** Location and function of the human frontal eye-field: a selective review.
762 *Neuropsychologia* 34: 475-483, 1996.
763 **Picard N, Strick PL.** Imaging the premotor areas. *Curr Opin Neurobiol* 11: 663–
764 672, 2001.
765 **Pierrot-Deseilligny C, Milea D, Müri RM.** Eye movement control by the
766 cerebral cortex. *Curr Opin Neurol* 17: 17-25, 2004.
767 **Robinson DA, Fuchs AF.** Eye movements evoked by stimulation of frontal eye
768 fields. *J Neurophysiol* 32: 637-648, 1969.
769 **Russo GS, Bruce CJ.** Supplementary eye field: representation of saccades
770 and relationship between neural response fields and elicited eye
771 movements. *J Neurophysiol* 84: 2605-2621, 2000.
772 **Schall JD.** Neuronal-Activity Related to Visually Guided Saccadic Eye-
773 Movements in the Supplementary Motor Area of Rhesus-Monkeys. *J*
774 *Neurophysiol* 66: 530-558, 1991.
775 **Schlag J, Schlag-Rey M.** Evidence for a supplementary eye field. *J*
776 *Neurophysiol* 57: 179–200, 1987.
777 **Schluppeck D, Glimcher P, Heeger DJ.** Topographic organization for delayed
778 saccades in human posterior parietal cortex. *J Neurophysiol* 94: 1372-
779 1384, 2005.
780 **Serences JT.** A comparison of methods for characterizing the event-related
781 BOLD timeseries in rapid fMRI. *Neuroimage* 21: 1690-1700, 2004.

782 **Sereno MI, Pitzalis S, Martinez A.** Mapping of contralateral space in
783 retinotopic coordinates by a parietal cortical area in humans. *Science* 294:
784 1350-1354, 2001.
785 **Sereno MI, Huang RS.** A human parietal face area contains aligned head-
786 centered visual and tactile maps. *Nat Neurosci* 9: 1337-1343, 2006.
787 **Soechting JF, Flanders M.** Moving in three-dimensional space: frames of
788 reference, vectors, and coordinate systems. *Annu Rev Neurosci* 15: 167–
789 191, 1992.
790 **Stuphorn V, Brown JW, Schall JD.** Role of supplementary eye field in
791 saccade initiation: executive not direct control. *J Neurophysiol* 103: 801-
792 816, 2010.
793 **Summerfield C, Monti JMP, Trittschuh EH, Mesulam MM, Egner T.** Neural
794 repetition suppression reflects fulfilled perceptual expectations. *Nat*
795 *Neurosci* 11: 1004-1006, 2008.
796 **Talairach J, Tournoux PA.** *A co-planar stereotaxic atlas of the human brain.*
797 New York: Thieme Medical Publishers, 1988.
798 **Tehovnik EJ, Lee K.** The dorsomedial frontal cortex of the rhesus monkey:
799 topographic representation of saccades evoked by electrical stimulation.
800 *Exp Brain Res* 96: 430–442, 1993.
801 **Van Turennout M, Bielamowicz L, Martin A.** Modulation of neural activity
802 during object naming: effects of time and practice. *Cereb Cortex* 13: 381-
803 391, 2003.
804 **Vaziri S, Diedrichsen J, Shadmehr R.** Why does the brain predict sensory
805 consequences of oculomotor commands? Optimal integration of the

806 predicted and the actual sensory feedback. *J Neurosci* 26: 4188-4197,
807 2006.
808 **Vidyasagar R, Stancak A, Parkes LM.** A multimodal brain imaging study of
809 repetition suppression in the human visual cortex. *Neuroimage* 49: 1612-
810 1621, 2010.
811 **Wiggs CL, Martin A.** Properties and mechanisms of perceptual priming. *Curr*
812 *Opin Neurobiol* 8: 227-233, 1998.
813
814
815

816 **Figure legends**

817

818 Figure 1.

819 *A*. Experimental paradigm. *Upper panel.* A typical novel trial *t* started with the
820 illumination of a fixation LED (F). After 3 s, a saccadic target LED (S) was
821 flashed for 200 ms in the visual periphery, while subjects kept fixation at F. After
822 a memory delay period of 3.8 s, F was extinguished, which cued the subject to
823 make a saccade to S. 1 s later the next trial started. *Lower panels*. In a
824 subsequent repetition trial *t+1*, S could be presented at either the same retinal
825 location as in the previous trial, while the location was novel in non-retinal
826 (head-centered) coordinates (left), or at a novel retinal position, but at the same
827 non-retinal location (right). Alternatively, the targets location could be either
828 novel or repeated in both coordinate frames (not shown). Both fixation and
829 target stimulus LEDs were yellow-colored and had the same luminance
830 (difference in LED luminance in the figure is for clarification purposes only). *B*.
831 Eye traces of one subject over the time course of 20 trials with F at 0° and S
832 either at -9° (black traces) or 9° (gray traces). The subject keeps fixation
833 throughout the trial, also during target stimulus presentation. After the go cue,
834 response saccades are consistently made toward the location of the
835 remembered target.

836

837

838 Figure 2.

839 Brain activation during the oculomotor network localizer trials, averaged across
840 all 18 subjects ($P<0.01$, FDR-corrected; 25 mm^2 cluster threshold). Data are

841 presented in 2 anatomical views in neurological convention (*A*, *B*), and on an
842 inflated representation of the left hemisphere of one of the subjects (*C*, *D*). A
843 parietofrontal network is activated, including areas on the banks of the
844 intraparietal sulcus (IPS), the frontal eye field (FEF), supplementary eye fields
845 (SEF) and the left ventral premotor area (PMv).
846
847 Figure 3.
848 Group results. *A,B.* Reconstruction of the hemodynamic responses (in pseudo
849 z-values, referred to as arbitrary units (a.u.)) in the IPS averaged across all
850 subjects, for novel (black traces) and repeated trials (gray traces) in retinal (A)
851 and non-retinal (B) coordinates. C, D. Average difference between repeated
852 and novel trials, together with 95% confidence intervals. LH, left hemisphere;
853 RH, right hemisphere. Gray areas indicate the periods over which the
854 differences between the novel and repeated trials were taken. S, Stimulus; D,
855 Delay; E, Execution phase.
856
857 Figure 4.
858 Repetition suppression effects in the IPS, FEF, and SEF, at various trial phases
859 in relation to a retinal (black bars) and non-retinal (white bars) reference frame.
860 Data (in a.u.) combined across hemispheres. Error bars: SE. * $P<0.05$; **
861 $P<0.01$, *** $P<0.001$.
862
863 Figure 5.
864 Indexing the spatial reference frames across the population of subjects, in the
865 IPS, FEF, and SEF during the same epochs as in Figure 4. Reference Frame

866 Index (RFI) was computed as the difference between the amount of retinal and
867 non-retinal RS, normalized by the total amount of RS. Positive values indicate a
868 dominance of retinal coding, negative values point to non-retinal coding. In all
869 cases, average RFI across the population is larger than zero ($p<0.01$).
870
871 Figure 6.
872 Lateralized activity in IPS, FEF and SEF during the delay period, averaged
873 across subjects. *A*. Difference in BOLD signal (in a.u.), across hemispheres,
874 between contralateral and ipsilateral target locations in retinal coordinates. A
875 contralateral bias exists in the IPS and FEF ($P<0.001$), but not in the SEF
876 ($P=0.78$). *B.* Lateralized activity when target locations are expressed in terms of
877 their non-retinal location. No directional preference for non-retinal targets is
878 observed in any of the regions. Error bars: SE.
879
880

881 **Tables**

882

883 Table 1. Percentage correct responses (% ± SD) and mean reaction times (RT

884 ± SD, ms) for each of the four conditions.

Target Location Condition	Performance (%)	RT (ms)
Novel retinal, novel non-retinal	94.5 ± 5.3	215 ± 69
Repeated retinal, novel non-retinal	93.8 ± 7.3	220 ± 74
Novel retinal, repeated non-retinal	94.7 ± 6.2	215 ± 83
Repeated retinal, repeated non-retinal	96.3 ± 3.5	220 ± 64

885

886

887 Table 2. Brain regions activated during saccade planning and execution.

888 Coordinates in mm: x (lateral/medial), y (anterior/posterior) and z

889 (superior/inferior), according to Talairach and Tournoux (Talairach and

890 Tournoux 1988). The t-values represent each area's peak voxel statistic across

891 all subjects.

Anatomical Region	Functional Label	Side	x	y	z	t-Value
Intraparietal sulcus	IPS	L	-18	-59	49	9.60
		R	14	-61	52	7.10
Superior frontal sulcus	FEF	L	-25	-10	53	8.45
		R	21	-6	53	5.81
Medial frontal cortex	SEF	L	-1	-4	57	11.25
		R	2	-4	57	11.26
Precentral sulcus	PMv	L	-55	-2	38	5.73

892

893

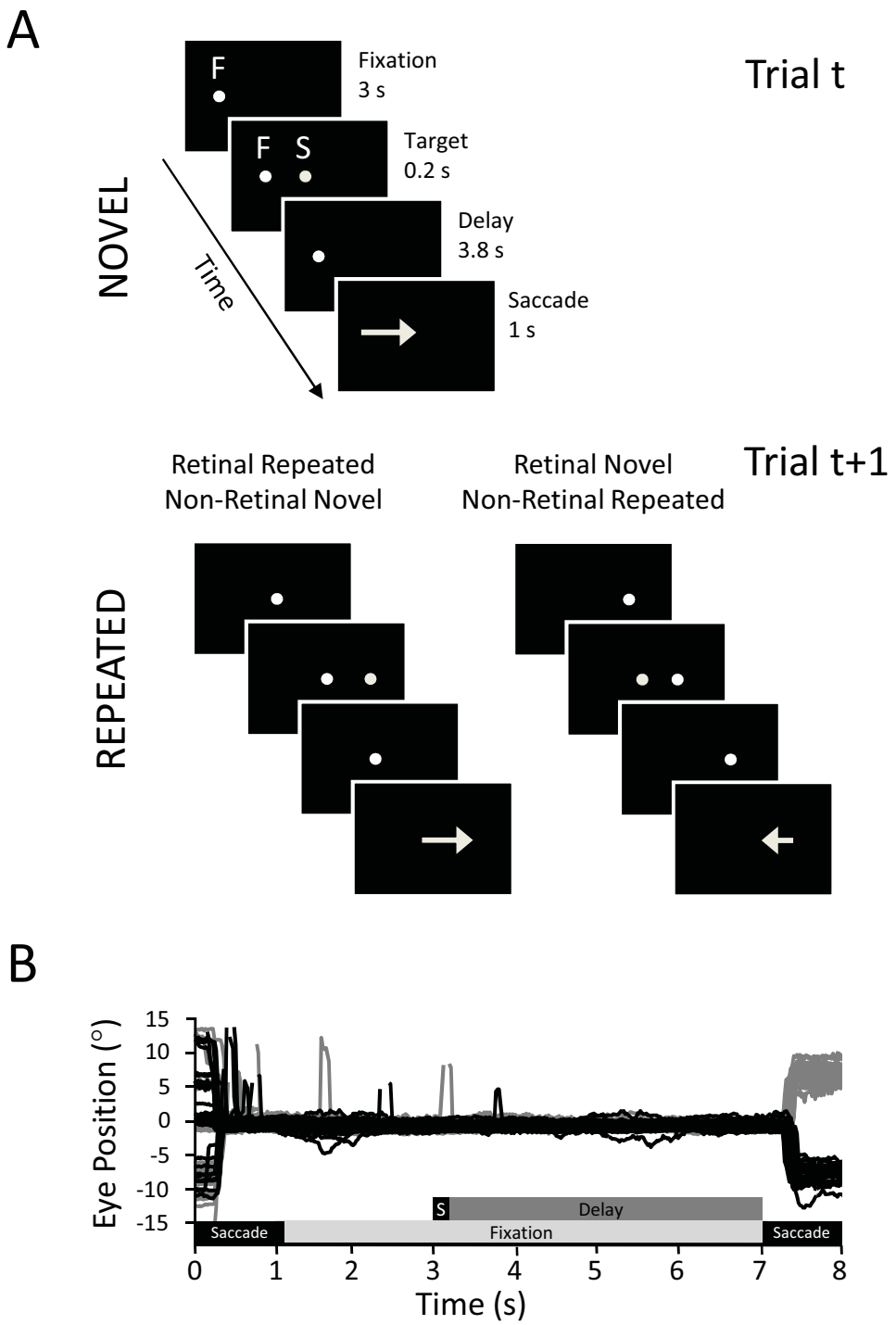
A
Trial t
F
Fixation
3 s
F S
Target
0.2 s
Delay
3.8 s
Saccade
1 s
NOVEL
Time
Trial t+1
Retinal Repeated
Non-Retinal Novel
Retinal Novel
Non-Retinal Repeated
REPEATED
B
Eye Position (°)
15
10
5
0
-5
-10
-15
S
Delay
Saccade
Fixation
Saccade
0
1
2
3
4
5
6
7
8
Time (s)

FIGURE 1

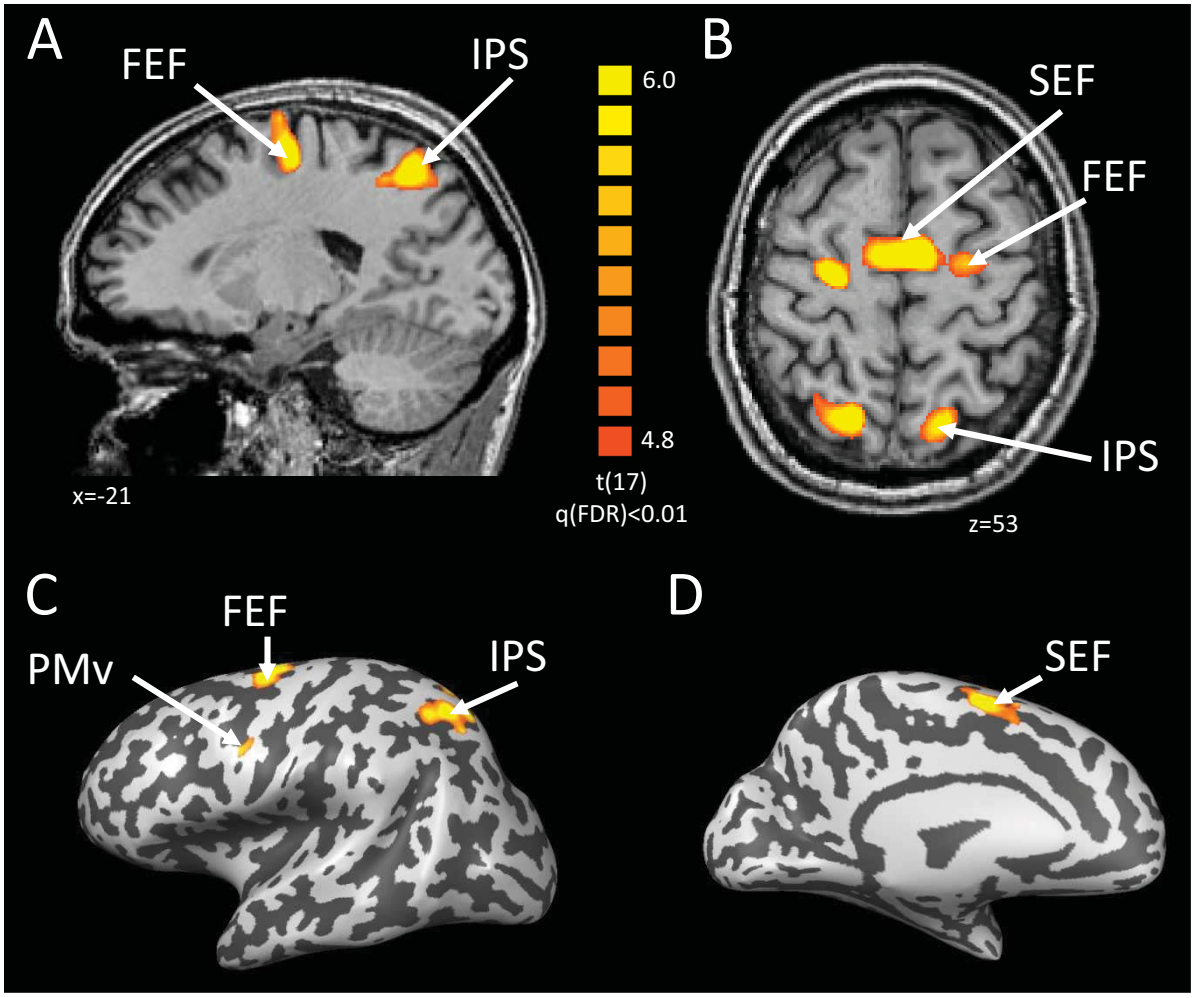
A
FEF
IPS
x=-21
6.0
4.8
t(17)
q(FDR)<0.01
B
SEF
FEF
IPS
z=53
C
FEF
PMv
IPS
D
SEF

FIGURE 2

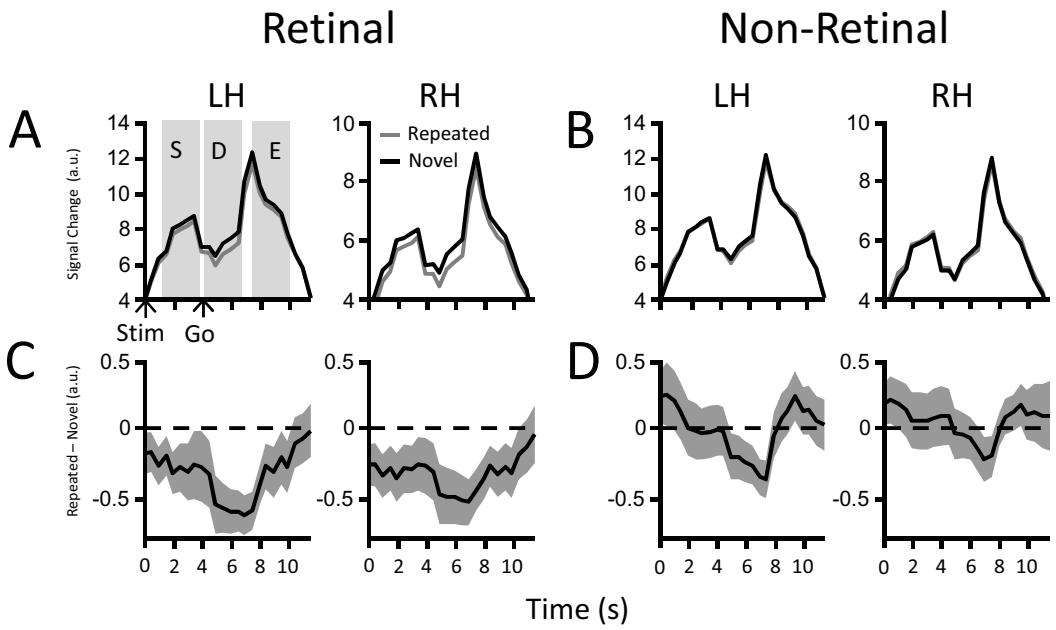
Retinal
Non-Retinal
A
B
C
D
LH
RH
LH
RH
S
D
E
Repeated
Novel
Signal Change (a.u.)
Stim
Go
Repeated – Novel (a.u.)
Time (s)

FIGURE 3

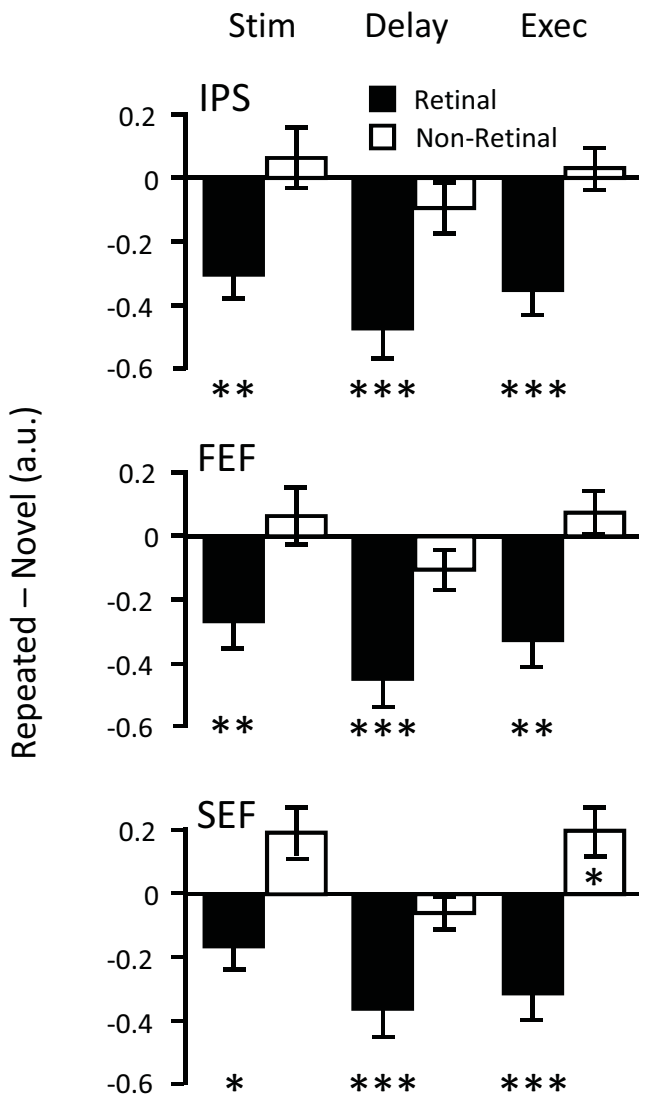
Stim
Delay
Exec
IPS
Retinal
Non-Retinal
0.2
0
-0.2
-0.4
-0.6
**
***
***
FEF
0.2
0
-0.2
-0.4
-0.6
**
***
**
SEF
0.2
0
-0.2
-0.4
-0.6
*
*
***
***
Repeated – Novel (a.u.)

FIGURE 4

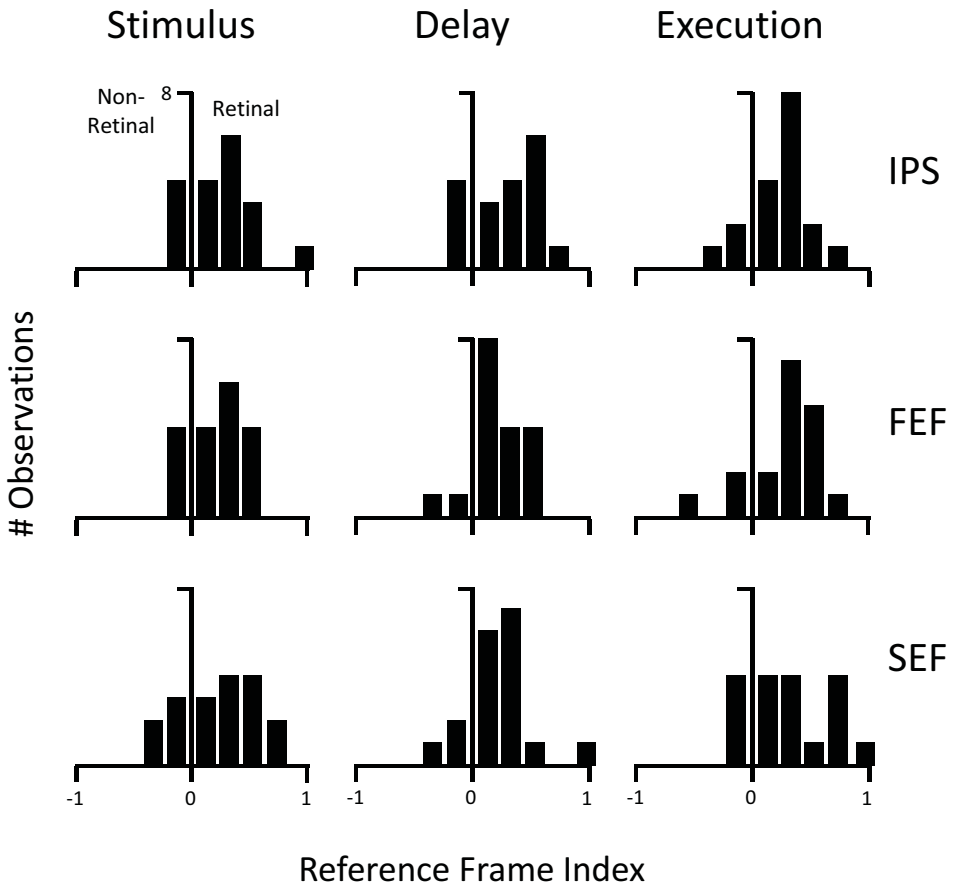
Stimulus
Delay
Execution
Non-
Retinal
8
Retinal
IPS
FEF
SEF
Observations
-1
0
1
-1
0
1
-1
0
1
Reference Frame Index

FIGURE 5

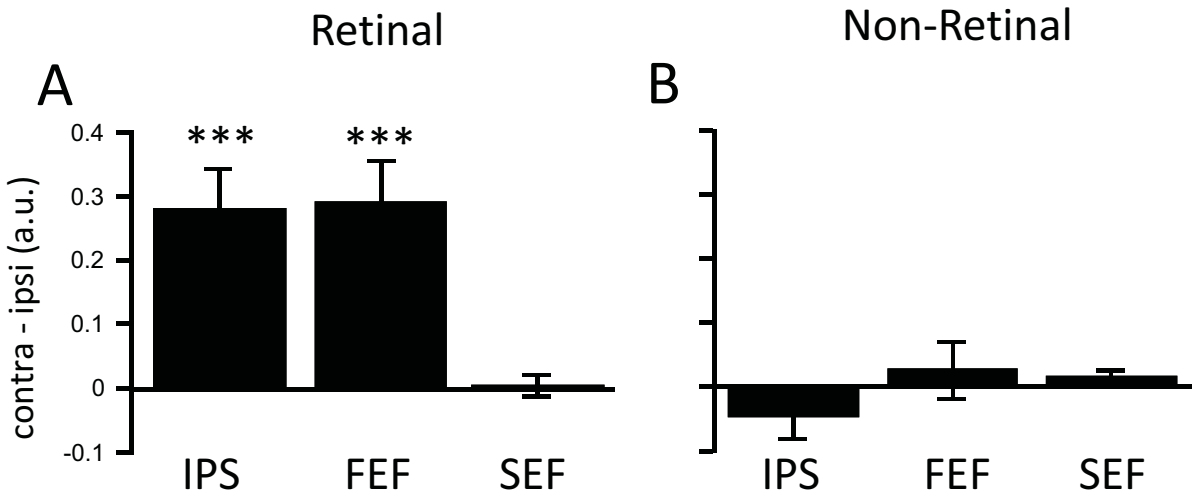
Retinal
Non-Retinal
A
B
***
***
0.4
0.3
0.2
0.1
0
-0.1
contra - ipsi (a.u.)
IPS
FEF
SEF
IPS
FEF
SEF

FIGURE 6